Exploring the transition from BCS to unitarity using normal modes: energies, entropies, critical temperatures and excitation frequencies

D. K. Watson

Homer L. Dodge Department of Physics and Astronomy, University of Oklahoma, Norman, 73019, Oklahoma, USA.

Contributing authors: dwatson@ou.edu;

ORCID iD: D.K. Watson https://orcid.org/0000-0001-8678-7745
Acknowledgments: This research was funded by the National Science Foundation under Grant No. PHY-2011384.

1 Introduction

The BCS to unitarity transition for ultracold gaseous fermions has been investigated intensely both experimentally and theoretically since this transition was first achieved in the laboratory[1–9]. Theoretical methods typically assume that the atomic fermions form Cooper pairs to explain the emergence of superfluid behavior[10–16]. When a Feshbach resonance is tuned to weak interactions, the neutral atoms bind into loosely-bound pairs whose size decreases as the interparticle interaction strength increases toward unitarity. Eventually diatomic molecules are produced that condense in the BEC regime. In materials that support superconductivity, the binding of electrons into Cooper pairs at long distances is thought to be mediated by phonon interactions in the underlying material producing a weak attraction[10–14].

The ability of normal modes to describe superfluidity in the strongly interacting unitary regime has previously been investigated for ultracold Fermi gases[17, 18], obtaining results for ground state energies comparable to benchmark results[17] and thermodynamic quantities in excellent agreement with

experiment[18]. The current study tests this normal mode picture away from unitarity. A preliminary study was completed that looked at the behavior of the N -body analytic normal mode frequencies from the BCS regime to unitarity[19]. This study confirmed behavior seen in the laboratory with the emergence of excitation gaps that increased from extremely small gaps deep in the BCS regime to a maximum at unitarity. The microscopic dynamics responsible for the emergence of these gaps was investigated using the analytic forms of the normal mode functions and a microscopic basis for universal behavior at unitarity was proposed.

In this paper, I now explore the ability of these normal modes to describe observables away from the strongly interacting unitary regime including ground state energies, thermodynamic entropies, critical temperatures, and the breathing excitation frequency. This approach models the physics by assuming many-body pairing manifested through normal modes, i.e. coherent, collisionless motion of the fermions that minimizes interparticle interactions and makes two-body pairing irrelevant since it is impossible to discern which fermion is paired with another fermion. Normal mode functions naturally provide simple, coherent macroscopic wave functions that maintain phase coherence over the whole ensemble, and give rise to "quasiparticles" defined by the excitations between the modes.

Normal mode motions exist at all scales in our universe from vibrating crystals[20] to oscillating black holes[21]. The particles in a normal mode move in synchrony with the same frequency and phase, allowing a description of the complex, simultaneous motions of many interacting particles in terms of collective behavior. These modes are a manifestation of the widespread appearance of vibrational motions that occur in nature in diverse media and across many orders of magnitude[20–32]. When higher-order effects are small, vibrational behavior couples into stable collective motion, thus incorporating the many-body effects of large ensembles into simple dynamic motions. These collective motions correspond to the eigenfunctions of an approximate Hamiltonian and thus possess some stability over time. Normal modes reflect the symmetry that is present in this approximate Hamiltonian and can offer beyond-mean-field analytic many-body solutions and physical intuition into the microscopic dynamics responsible for diverse phenomena.

2 Symmetry-Invariant Perturbation Theory: A Group Theoretic and Graphical Approach

2.1 Background

The formalism used to obtain these normal modes is called symmetry-invariant perturbation theory (SPT), a first-principle, non-numerical method that uses group theoretic and graphical techniques to solve many-body problems[33–38]. This method, which has no adjustable parameters, uses the inverse dimensionality of space as the perturbation parameter. The study of physical systems

using $1/D$ or $1/N$ expansions was originally developed in quantum chromodynamics by t'Hooft[39], and was subsequently used in condensed matter by Wilson[40] to determine critical exponents for $D = 3$ phase transitions starting from exact values at $D = 4$. Dimensional expansion techniques are now found in many areas of physics including atomic[41–47] and molecular physics[41–43, 48–59], Bose gases[60–62], as well as Fermi gases in the unitary regime[63–66], relativistic quantum systems[67–71], nuclear physics[72, 73], quantum field theory[74–80], condensed matter physics[40, 81–83], and statistical physics[84, 85] among others.

The SPT formalism used in the current study was developed to handle the large systems of particles being studied in the atomic physics/condensed matter communities at ultracold temperatures, initially applied to bosonic systems[33–36, 62] and more recently to ultracold Fermi gases[17, 18] requiring the enforcement of the Pauli principle[17, 18, 86, 87]. The current version has been formulated through first order for $L = 0$, three-dimensional systems with completely general interaction potentials and spherically-symmetric confining potentials. Unlike conventional methods for which the resources for an exact solution of the quantum N -body wave function scale exponentially with N , typically doubling for every particle added[88, 89], the SPT approach employs symmetry to attack the N -scaling problem[33–35]. This is accomplished by formulating a perturbation series about a large-dimension configuration whose point group is isomorphic to the symmetric group S_N , and then evaluating the series for $D = 3$. The perturbation terms are evaluated for large dimension where the structure has maximum symmetry yielding terms that are invariant under the $N!$ operations of the S_N point group. This strategy produces a problem order-by-order that no longer scales with N [90, 91], and in principle, can be solved exactly, analytically using symmetry. Although extremely challenging, the mathematical work at each order can be saved[92] and used to study a problem with a new interaction potential significantly reducing numerical demands.

Even at the lowest perturbation order, the SPT method includes beyond-mean-field effects that underlie the excellent results achieved at first order using this SPT method[17, 18, 62] as well as earlier dimensional approaches[93–97]. This formalism has also been implemented for a model problem of harmonically-confined, harmonically-interacting particles that is exactly solvable[37, 38, 86, 87]. Accuracy of ten or more digits was found for the wave function compared to the exact wave function obtained independently, verifying this general many-body formalism for a three-dimensional, many-body system that is fully-interacting [37] including the formulas derived analytically for the N-body normal mode coordinates and frequencies.

Initial studies of fermionic systems focused on the unitary regime. The heavy numerical demands of enforcing antisymmetry in fermion systems in conventional theoretical approaches are avoided in the SPT approach by enforcing the Pauli principle "on paper" using specific occupations of the normal modes at first order[17, 18, 86, 87]. (See Section 2.2.4.) Beyond-mean-field ground[17]

and excited state[18] energies and their degeneracies have been calculated enabling the determination of a partition function and the calculation of thermodynamic quantities[18, 87]. An accurate partition function requires many states chosen from the infinite spectrum by the Pauli principle, thus relating the Pauli principle to many-body interaction dynamics through the normal modes.

The physical character of the analytic normal mode coordinates was investigated as a function of N with the goal of obtaining insight into the microscopic dynamics of cooperative motion[98] and the universal behavior at unitarity. This study found a smooth evolution as N increases from the expected behavior for few-body systems whose motions are analogous to those of molecular equivalents such as ammonia and methane, to the coherent motions observed in large N ensembles. Furthermore, the transition from few-body to large N behavior occurs at surprisingly low values of N ($N \approx 10$) validating the results of numerous few-body studies[99–106]. This evolution in character from few-body to large ensembles is dictated by rather simple analytic forms that nevertheless take into account the complicated interplay of the particles as they interact and cooperate to create coherent macroscopic motion. This behavior was dependent primarily on the symmetry present in the Hamiltonian, and thus could be relevant for diverse phenomena at different scales if the same symmetry exists or is dominant.

In the current paper, I now investigate whether these first-order normal mode solutions can accurately determine observables away from universal behavior of the strongly interacting unitary regime.

2.2 The SPT formalism

This section contains a brief summary of the SPT formalism. More detailed summaries can be found in Refs. [18, 19].

2.2.1 The Hamiltonian

For N interacting particles, the Schrödinger equation in D dimensions is:

$$H\Psi = \left[\sum_{i=1}^{N} h_i + \sum_{i=1}^{N-1} \sum_{j=i+1}^{N} g_{ij} \right] \Psi = E\Psi \,, \tag{1}$$

$$\begin{aligned} h_i &= -\frac{\sim^2}{2m_i} \sum_{\nu=1}^{D} \frac{\partial^2}{\partial x_{i\nu}^2} + V_{\text{conf}} \left(\sqrt{\sum_{\nu=1}^{D} x_{i\nu}^2} \right) \,, \\ g_{ij} &= V_{\text{int}} \left(\sqrt{\sum_{\nu=1}^{D} (x_{i\nu} - x_{j\nu})^2} \right) \,, \end{aligned} \tag{2}$$

where h_i is the single-particle Hamiltonian, g_{ij} a two-body interaction potential, $x_{i\nu}$ the ν^{th} Cartesian component of the i^{th} particle, and V_{conf} is a spherically-symmetric confining potential[33–35]. Defining internal coordinates as the D-dimensional scalar radii r_i of the N particles from the center of the

trap and the cosines γ_{ij} of the $N(N-1)/2$ interparticle angles between the radial vectors:

$$\begin{aligned} r_i &= \sqrt{\sum_{\nu=1}^{D} x_{i\nu}^2}, \quad (1 \le i \le N), \\ \gamma_{ij} &= \cos(\theta_{ij}) = \sum_{\nu=1}^{D} x_{i\nu} x_{j\nu} \Big/ r_i r_j , \end{aligned} \tag{3}$$

$(1 \le i < j \le N)$, the Schrödinger equation is transformed from Cartesian to internal coordinates.

A scale factor, $\kappa(D) = D^2 \bar{a}_{ho}$, with $\bar{a}_{\rm ho} = \sqrt{\frac{\hbar}{m\omega_{\rm ho}}}$ and $\bar{\omega}_{\rm ho} = D^3 \omega_{\rm ho}$, is used to regularize the large-dimension limit by defining dimensionally-scaled oscillator units. Substituting scaled variables, $\bar{r}_i = r_i/\kappa(D)$, with $\bar{E} = \frac{E}{\hbar\bar{\omega}_{\rm ho}}$ and $\bar{H} = \frac{H}{\hbar\bar{\omega}_{\rm ho}}$ into the similarity-transformed Schrödinger equation[34, 107] and defining $\delta = 1/D$ and $\hbar = m = 1$ gives:

$$\bar{H}\Phi = \delta^2 \bar{T} + \bar{U} + \bar{V}_{\rm conf} + \bar{V}_{\rm int}\,\Phi = \bar{E}\,\Phi . \tag{4}$$

where

$$\bar{T} = \sum_{i=1}^{N} \left(-\frac{1}{2}\frac{\partial^2}{\partial \bar{r}_i^{\,2}} - \frac{1}{2\bar{r}_i^{\,2}} \sum_{j\neq i} \sum_{k\neq i} \frac{\partial}{\partial\gamma_{ij}} (\gamma_{jk} - \gamma_{ij}\gamma_{ik}) \frac{\partial}{\partial\gamma_{ik}} \right) , \tag{5}$$

$$\bar{U} = \sum_{i=1}^{N} \frac{\delta^2 N(N-2) + (1-\delta(N+1))^2 \left(\frac{\Gamma^{(i)}}{\Gamma}\right)}{8\bar{r}_i^{\,2}} , \tag{6}$$

$$\bar{V}_{\rm conf} = \sum_{i=1}^{N} \frac{1}{2}\bar{r}_i^{\,2} \tag{7}$$

$$\bar{V}_{\rm int} = \frac{\bar{V}_0}{1 - 3b'\delta} \sum_{i=1}^{N-1} \sum_{j=i+1}^{N} (1 - \tanh\Theta_{i,j}) , \tag{8}$$

and Γ is the Gramian determinant with elements γ_{ij}, and $\Gamma^{(i)}$ is the determinant with the i^{th} row and column deleted. The barred quantities are scaled by $\kappa(D)$. The interaction potential, $\bar{V}_{\rm int}$, reduces to a square well for $D = 3$. The value of the constant b' yields a scattering length of infinity when $\bar{V}_0 = 1.0$. $\bar{V}_0$ is scaled to smaller values to reach the weaker interactions of the BCS regime. The argument $\Theta_{ij} = \frac{c_0}{1-3\delta}\left(\bar{r}_{ij}\sqrt{\frac{}{2}}\,\bar{\alpha} - 3\delta\,\bar{R} - \bar{\alpha}\right)$ where $\bar{r}_{ij} = \sqrt{\bar{r}_i^{\,2} + \bar{r}_j^{\,2} - 2\bar{r}_i\bar{r}_j\gamma_{ij}}$ is the interatomic separation, $\bar{R}$ is the dimensionally-scaled range of the square-well potential, and $\bar{\alpha}$ is a constant that softens the

potential as $D \to \infty$. R is selected so $R << a_{ho}$ ($a_{ho} = \sqrt{\hbar/(m\omega_{ho})}$) and is extrapolated to zero-range interaction.

At the $D \to \infty$ limit, the second derivative terms of the kinetic energy drop out resulting in a static zeroth-order problem with an effective potential, $\bar{V}_{\rm eff}$:

$$\bar{V}_{\rm eff}(\bar{r}, \gamma; \delta) = \sum_{i=1}^{N} \bar{U}(\bar{r}_i; \delta) + \bar{V}_{\rm conf}(\bar{r}_i; \delta) + \sum_{i=1}^{N-1} \sum_{j=i+1}^{N} \bar{V}_{\rm int}(\bar{r}_i, \gamma_{ij}; \delta). \tag{9}$$

The minimum of $\bar{V}_{\rm eff}$ corresponds to a large-dimension maximally-symmetric configuration with all radii, $\bar{r}_i$, and angle cosines, γ_{ij}, of the particles equal, i.e. when $D \to \infty$, $\bar{r}_i = \bar{r}_\infty$ $(1 \le i \le N)$ and $\gamma_{ij} = \gamma_\infty$ $(1 \le i < j \le N)$.

2.2.2 The Dimensional Expansion

The energy minimum as $\delta \to 0$, $\bar{E}_\infty$, is the starting point for the $1/D$ expansion. The $N(N+1)/2$ internal coordinates, $\bar{r}_i$ and γ_{ij}, are expanded as: $\bar{r}_i = \bar{r}_\infty + \delta^{1/2}\bar{r}'_i$ and $\gamma_{ij} = \gamma_\infty + \delta^{1/2}\vec{\gamma}_{ij}$ setting up a power series in $\delta^{1/2}$ about the $D \to \infty$ symmetric minimum. The primed variables, $\bar{r}'_i$ and $\vec{\gamma}_{ij}$, are dimensionally-scaled internal *displacement* coordinates. Expansions of the Hamiltonian, wave function, and energy in powers of $\delta^{1/2}$ are:

$$\begin{aligned} \bar{H} &= \bar{H}_\infty + \delta^{\frac{1}{2}}\bar{H}_{-1} + \delta \sum_{j=0} \left(\delta^{\frac{1}{2}}\right)^j \bar{H}_j \\ \Phi(\bar{r}_i, \gamma_{ij}) &= \sum_{j=0} \left(\delta^{\frac{1}{2}}\right)^j \Phi_j \\ \bar{E} &= \bar{E}_\infty + \delta^{\frac{1}{2}}\bar{E}_{-1} + \delta \sum_{j=0} \left(\delta^{\frac{1}{2}}\right)^j \bar{E}_j, \end{aligned} \tag{10}$$

where

$$\bar{H}_\infty = \bar{E}_\infty \tag{11}$$

$$\bar{H}_{-1} = \bar{E}_{2n-1} = 0, \tag{12}$$

$$\bar{H}_0 = -\frac{1}{2}{}^{(0)}_2 G_{\nu_1,\nu_2} \frac{\partial}{\partial \bar{y}'_{\nu_1}} \frac{\partial}{\partial \bar{y}'_{\nu_2}} + \frac{1}{2}{}^{(0)}_2 F_{\nu_1,\nu_2} \bar{y}'_{\nu_1} \bar{y}'_{\nu_2} + {}^{(0)}_0 F, \tag{13}$$

$$\bar{H}_1 = -\frac{1}{2}{}^{(1)}_3 G_{\nu_1,\nu_2,\nu_3} \bar{y}'_{\nu_1} \frac{\partial}{\partial \bar{y}'_{\nu_2}} \frac{\partial}{\partial \bar{y}'_{\nu_3}} - \frac{1}{2}{}^{(1)}_1 G_{\nu} \frac{\partial}{\partial \bar{y}'_{\nu}} + \frac{1}{3!}{}^{(1)}_3 F_{\nu_1,\nu_2,\nu_3} \bar{y}'_{\nu_1} \bar{y}'_{\nu_2} \bar{y}'_{\nu_3} + {}^{(1)}_1 F_{\nu} \bar{y}'_{\nu}, \tag{14}$$

and the $\bar{y}'_{\nu i}$ are the components, $\bar{r}'_i$ and $\bar{\gamma}'_{ij}$, of the vector of dimensionally-scaled internal displacement coordinates (See Eqs. (17)-(18) in Ref. [18].)

$$\bar{y}' = \begin{matrix} \bar{r}' \\ \bar{\gamma}' \end{matrix} , \tag{15}$$

The superprescript on the F and G tensors in Eqs. (13)-(14) denotes the order in $\delta^{1/2}$ in the sum over j in Eq. (10). The subprescripts indicate the rank, R, of the tensors. The G elements are defined from the first-order derivative terms, $\bar{T}$, of the Hamiltonian while the F elements contain the first-order potential terms from $\bar{V}_{\text{eff}}$. Appendix B of Ref. [62] gives formulas for the F and G elements.

2.2.3 Symmetry Coordinates and Normal Modes

According to Eqs. (10) and (13), $\bar{H}_0$ contains contributions from all terms in the Hamiltonian, including the interparticle interaction, through first order in the displacements from the maximally-symmetric structure. $\bar{H}_0$ has the form of a multidimensional harmonic oscillator, so the first-order wave function can be expressed in terms of the normal mode basis whose frequencies and coordinates include effects of the many-body interactions of the particles through first order. Since $\bar{H}_0$ is invariant under S_N, the normal modes transform under irreducible representations (irreps.) of the S_N group. For the $\bar{r}'$ vector, the irreps. are $[N]$ and $[N-1,\,1]$, while for the $\bar{\gamma}'$ vector, the irreps. are $[N]$, $[N-1,\,1]$, and $[N-2,\,2]$.

The normal mode coordinates and their frequencies are obtained using a quantum chemistry method, the FG method developed by Wilson in 1941[108], which has been used extensively to study molecular normal mode behavior[109]. The determination of the normal modes coordinates[34] and their frequencies[33] was achieved analytically using group theoretic techniques. The five irreducible representations of S_N[110, 111] are labelled $0^+, 0^-, 1^+, 1^-, 2$[33] where the $N(N-3)/2$ normal modes of type 2 are phonon modes; the $N-1$ modes of type 1^- exhibit single-particle i.e. particle-hole radial excitation behavior; the $N-1$ normal modes of type 1^+ have single-particle/particle-hole angular excitation behavior; the single 0^+ normal mode is a symmetric bend/center of mass motion, and the single 0^- normal mode is a symmetric stretch/ breathing motion. These motions are analyzed in detail in Ref. [98]. The energy through first order in $\delta = 1/D$ is: [33]

$$\bar{E} = \bar{E}_\infty + \delta \sum_{\mu=\{0^\pm,\ 1^\pm,\ 2\}} (n_\mu + \frac{1}{2} d_\mu)\bar{\omega}_\mu + v_o \ , \tag{16}$$

where n_μ is the total normal mode quanta with frequency $\bar{\omega}_\mu$; μ the normal mode label ($0^+, 0^-, 1^+, 1^-, 2$), and v_o a constant. The multiplicities are: $d_{0^+} = 1,\ d_{0^-} = 1,\ d_{1^+} = N-1,\ d_{1^-} = N-1,\ d_2 = N(N-3)/2$.

Normal modes for the $\alpha = [N]$ and $[N-1, 1]$ sectors in terms of symmetry coordinates $[S^{\alpha}_{X}]_{\xi}$ are given by: $q^{\alpha}_{\pm} = c^{\alpha}_{\pm} \cos\theta^{\alpha}_{\pm} [S^{\alpha}_{\overline{x}}]_{\xi} + \sin\theta^{\alpha}_{\pm} [S^{\alpha}_{\overline{Y}}]_{\xi}$ [34] where $\cos\theta^{\alpha}_{\pm}$ and $\sin\theta^{\alpha}_{\pm}$ are mixing coefficients and the $\pm$ refer to 0^{+} and 0^{-} for the $[N]$ sector and 1^{+} and 1^{-} for the $[N-1,1]$ sector. The 2 normal mode is: $q'^{[N-2,\ 2]} = c^{[N-2,\ 2]} S^{[N-2,\ 2]}_{\overline{Y}}$.

2.2.4 Applying the Pauli Priniple

The energy expression, Eq. (16), gives the energy of the ground state as well as the excited state spectrum. The Pauli allowed states are determined by setting up a correspondence between the states identified by normal mode quantum numbers $|n_{0^+}, n_{0^-}, n_{1^+}, n_{1^-}, n_2>$ and the non-interacting states of the trap with ν_i, the radial quantum number and l_i, the orbital angular momentum quantum number of the three dimensional harmonic oscillator ($V_{\text{conf}}(r_i) = \frac{1}{2}m\omega^2_{ho} r_i^2$). These single-particle quantum numbers satisfy $n_i = 2\nu_i + l_i$, where n_i is the ith particle energy level quanta defined by: $E = \sum_{i=1}^{N} \left[n_i + \frac{3}{2} \right] \hbar\omega_{ho} = \sum_{i=1}^{N} \left[(2\nu_i + l_i) + \frac{3}{2} \right] \hbar\omega_{ho}$. The states of the harmonic oscillator have known constraints due to antisymmetry that can be transferred to the normal mode representation in the double limit $D \to \infty$, $\omega_{ho} \to \infty$ where both representations are valid. The radial and angular quantum numbers separate at this double limit resulting in two conditions[17, 86]:

$$2n_{0^-} + 2n_{1^-} = \sum_{i=1}^{N} 2\nu_i, \quad 2n_{0^+} + 2n_{1^+} + 2n_2 = \sum_{i=1}^{N} l_i \tag{17}$$

Eqs. (17) define a possible set of normal mode states $|n_{0^+}, n_{0^-}, n_{1^+}, n_{1^-}, n_2>$ consistent with an antisymmmetric wave function from the set of harmonic oscillator configurations that are known to obey the Pauli principle. As particles are added at the non-interacting $\omega_{ho} \to \infty$ limit, additional harmonic oscillator quanta, ν_i and l_i, are, of course, required by the Pauli principle as fermions fill the harmonic oscillator levels. Equivalently, this corresponds to additional normal mode quanta required to ensure antisymmetry as the normal modes begin to reflect the emerging interactions. This strategy is analogous to Landau's use of the non-interacting system in Fermi liquid theory to set up the correct Fermi statistics as interactions evolve adiabatically[112].

3 Application: Ultracold Fermi Gases from BCS to Unitarity

I assume an N-body system of fermions, with equal numbers of "spin up" and "spin down" fermions and $L = 0$ symmetry. The particles are confined by a spherically-symmetric harmonic potential with frequency ω_{ho} so $a_{ho}(= \sqrt{\hbar/(m\omega_{ho})})$ and ω_{ho} are the characteristic length and energy scales of the trap, representing the largest length scale and smallest energy scale of

the problem. An attractive square-well potential of radius R is set up with a potential depth parameter $\bar{V}_0$ in scaled units which is varied from a value of 1.0 where the magnitude of the s-wave scattering length, a_s, is infinite to zero as the gas becomes weakly interacting in the BCS regime. The range is chosen such that $R \ll a_{ho}$.(See Eq. (8))

When the scattering length a_s is much smaller than the interparticle spacing the system is considered weakly interacting. To reach the strongly interacting unitary regime, a Feshbach resonance can be tuned using an external magnetic field so that the scattering length becomes much larger than the other length scales of the problem. The system is strongly interacting in this regime and is independent of the microscopic details acquiring universal behavior.

I apply the full SPT many-body formalism defining the internal displacement coordinates and determining symmetry coordinates, normal mode coordinates and frequencies as a function of N . The energy expression of Eq. (16) gives the ground state energy as well as the excited state spectrum used to construct the partition function. Values of N were chosen in the range $10 \leq N \leq 30$ which had produced excellent results in the unitary regime. For the thermodynamic quantities, converging the partition function for higher values of N becomes extremely difficult.

The canonical partition function is defined as: $Z = \sum_{j=0}^{\infty} g_j \exp(-E_j/T)$, where E_j is a many-body energy, T is the temperature ($k_B = 1$), and g_j is the degeneracy of E_j. To determine a particular degeneracy, I search for all the partitions of the N particles into different levels, n_i, $i = 1, , , N$ that yield the correct E_j. For each partition, I find the possible quantum numbers l_i and ν_i of the occupied sublevels for all possible particle arrangements. Gathering these statistics yields the degeneracy as well as the sums over l_i and ν_i for this partition. I then use Eq. (17) to assign the normal mode quantum numbers to ensure antisymmetry. The quanta corresponding to the lowest normal mode frequencies are selected to yield the lowest energy for each excited energy level. This gives occupation in n_2, the phonon modes, and in n_{1^-}, the particle-hole radial excitation modes, which have the lowest angular and radial frequencies respectively. The conditions are:

$$2n_{1^-} = \sum_{i=1}^{N} 2\nu_i, \qquad 2n_2 = \sum_{i=1}^{N} l_i \,. \tag{18}$$

Thus, the enforcement of the Pauli principle yields occupation in different normal modes for each state determining the energy as well as character of the state since the normal modes have clear dynamical motions[98].

3.1 Ground state energies from BCS to Unitarity

Ground states energies have been determined for trapped Fermi gases across the transition from BCS to unitarity using the SPT formalism. The SPT energies as a function of $\bar{V}_0$ are shown in Fig. 1 from a value of $\bar{V}_0 = 10^{-8}$ deep in

the BCS regime to a value of $\bar{V}_0 = 1.0$ at unitarity. The energies are normalized by the noninteracting energies, E_{NI}, and increase rather rapidly from the values at unitarity converging to the expected noninteracting energies, E_{NI} as $\bar{V}_0 \to 0$. The energies at unitarity were determined in a previous study[17] and compared to other theoretical values, agreeing closely with benchmark auxilliary Monte Carlo results[113] for $N \leq 30$.

Unlike many approaches in the literature that use the s-wave scattering length, a_s, to set up a contact interaction for the interparticle interaction, the SPT method does not explicitly use the scattering length to define the interaction term. (The square-well potential has a scattering length associated with it, however, the solution of the perturbation equations is only through first order, so the results reflect only the first order terms from this potential, not the full scattering length.) To compare to both experimental and theoretical results in the literature, I have used simple interpolation between the SPT ground state energies across the transition with ground state energies in the literature that have been obtained using an explicit scattering length in the interaction term. This connects the interaction parameter $\bar{V}_0$ used in my SPT calculation to a value of the scattering length in a study using an explicit scattering length in the interaction term. (Because these two parameters have very different ranges ($0 \leq \bar{V}_0 \leq 1.0$; $-\infty \leq a_s \leq 0$) determining a scale factor between the parameters is probably not as accurate as interpolation.)

I chose to use the ground state energies from a density functional calculation[114] which were obtained by fitting their interaction parameters to very accurate energies for the trapped superfluid both at unitarity[115, 116] and in the BCS regime[117]. In Fig. 2, the SPT energies are regraphed as a function of these interpolated scattering lengths, specifically as a function of $1/k_f\, a_s$ where k_f is the Fermi momentum, and compared with available theoretical results[118] (including the density functional results used for the interpolation[114]) and experimental results[119]. For the experimental results which are for potential energies across the transition, I have assumed that the virial theorem which is valid at unitarity and at the independent particle limit holds across the transition[114, 120]. Using the results of other energy studies across this transition for the interpolation yields comparable results as the close agreement in Fig. 2 would suggest.

3.2 Entropies from BCS to Unitarity

Although thermodynamic quantities have been well studied in the unitary regime, there are very few determinations of thermodynamic quantities across the BCS to unitarity transition. I have chosen to look at entropies across this transition since values for the entropy as a function of temperature have been calculated at several values of $1/k_f\, a_s$ using a T-matrix approach[121]. My approach uses a straightforward calculation of the partition function, summing over the spectrum of equally-spaced normal mode states that are chosen by the Pauli principle.

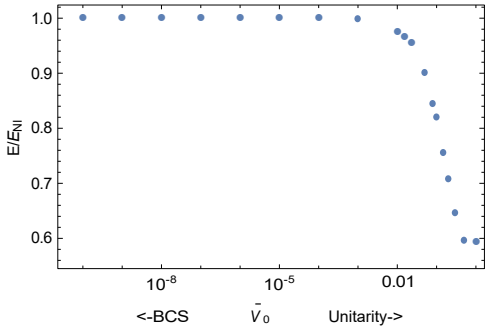

Fig. 1 The SPT ground state energies from BCS to unitarity as a function of $\bar{V}_0$ for $N = 12$.

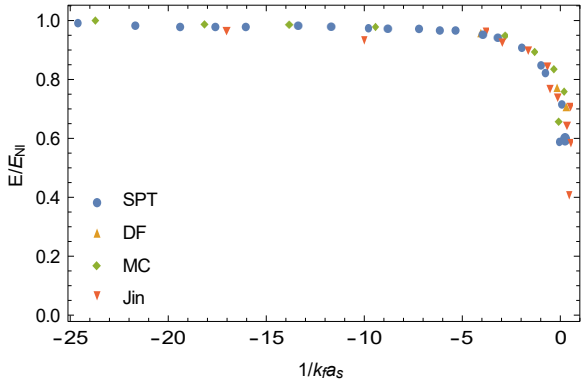

Fig. 2 Ground state energies from BCS to unitarity as a function of $1/k_f\, a_s$. My SPT results are for $N = 12$ and are compared to experimental [119], density functional (DF)[114] and variational Monte Carlo results (MC)[118].

In Fig. 3, I graph the entropy at $1/k_f\, a_s = -0.5$ comparing to the theoretical results of Ref. [121]. For comparison, using the interpolated values of the scattering length obtained above, I have plotted values for the entropy at unitarity, $1/k_f\, a_s = 0$ ($a_s = -\infty$), in Fig. 4 as a function of T/T_F (instead of the previous S vs. E plot in Ref. [18]).

The partition function becomes difficult to converge as the interparticle interaction decreases away from unitarity due to two effects: the narrowing of the frequencies and the increase in the value of the frequencies as they approach $2\omega_{ho}$ deep in the BCS regime. Larger frequency values mean that the individual terms of the partition function decrease their contribution to the total (a larger negative number in the numerator of each exponential) so more states are needed for convergence. The narrowing of the frequencies as the gaps shrink toward the BCS regime means that more states are becoming accessible at a given temperature which again increases the number of terms required for convergence. This increase in the number of states as interactions weaken results in higher entropy values as can be seen in Fig. 3 for the weaker interactions at $1/k_f a_s = -0.5$ compared to unitarity results in Fig. 4. The

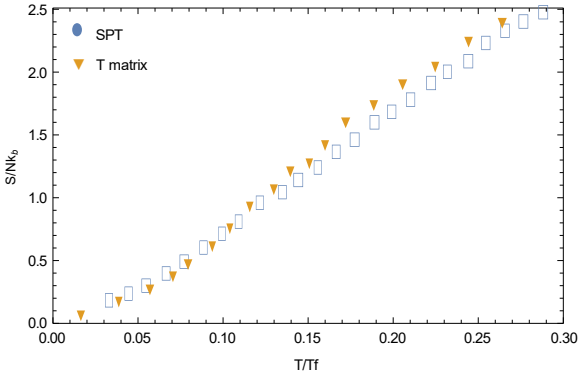

Fig. 3 The entropy for $N = 20$ as a function of T/T_F for $1/k_{fa} = -0.5$. SPT results - blue dots, T matrix results - orange triangles from Ref. [121]

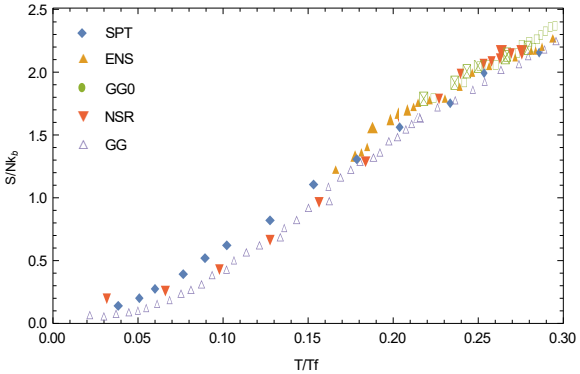

Fig. 4 The SPT entropy for $N = 20$ as a function of T/T_F at unitarity is compared to experimental data: ENS[122] and theoretical results: NSR, GG0, and GG[123, 128].

number of states needed also increases as the temperature increases. These three effects combine to make it very challenging to calculate thermodynamic quantities accurately across the BCS to unitarity transition using straightforward summing over the available states. Alternative approaches to obtaining a converged partition function are complicated by the need to enforce the Pauli principle at each step.

3.3 Estimate of Critical Temperatures from BCS to Unitarity

The critical temperature, T_C, is defined as the transition temperature from a normal fluid to a superfluid that exhibits long-range order due to a macroscopic occupation of the phonon ground state. This transition has been observed in the heat capacity whose thermodynamic expression involves a derivative with respect to the temperature. The heat capacity has a well-known, strong experimental signature in the unitary regime, the lambda transition, which has been

studied extensively both experimentally[4, 124–127] and theoretically[128–131]. An estimate of the critical temperature in the unitary regime has also been extracted from measurements of the entropy as a function of temperature using the thermodynamic relation; $1/T = \partial S/\partial E$[124].

Theoretically, the sudden change in thermodynamic properties as the ensemble becomes a superfluid is governed by the partition function and originates in the details of the lowest terms including the size of the gap and the degeneracies of the lowest states. For a given spectrum, the partitioning of particles among the available energy levels depends on a single parameter, the temperature. As the temperature drops below the critical temperature, one expects to see the occupation in the phonon ground state increase rapidly due to the gap in the spectrum. This phenomenon is manifested by a sudden change in the value of certain observables such as the specific heat.

In an earlier SPT study in the unitary regime[18], a calculation of the specific heat clearly showed a cusp at the lambda transition, yielding a critical temperature of $(T/T_F)_C = 0.16$ which was significantly lower than previous results in the literature for trapped Fermi gases: $(T/T_F)_C = 0.19$[122], 0.20[130], 0.21[128, 131, 132], $(T/T_F)_C = 0.27$[126, 129, 131], 0.29[124, 131].

In the current study, I have determined the specific heat for weaker interactions, $1/k_f a = -0.02$, $1/k_f a = -0.5$, and $1/k_f a = -1.0$, graphing the results in Fig. 5. As the interactions become weaker, the excitation gap decreases and the cusp signifying a transition to a superfluid quickly softens. While still visible at $1/k_f a = -0.02$ close to the unitary limit, the cusp is undetectable at a value of $1/k_f a \leq -0.5$ in the crossover region with only a slight inflection visible, and by $1/k_f a = -1.0$ no sign is detected. Thus, observing an experimental signature of this transition, certainly a definitive way to define the critical temperature, is not always possible in all regimes.

Theoretically, several approaches have been used to estimate the critical temperature at unitarity including a Monte Carlo study[130, 133] that uses the behavior of a correlation function to estimate the critical temperature, and an auxiliary field quantum Monte Carlo approach that determines the critical temperature from a change in the behavior of the thermodynamic energy as a function of temperature[129]. Along the entire transition from BCS to unitarity, the critical temperature has been calculated by solving the gap equation self-consistently with the number equation under the condition that the order parameter goes to zero as the temperature approaches the critical temperature, T_C, from below, i.e. long-range order is lost. These equations have been solved at different levels of approximation from mean field which yields the well known BCS results to solutions in strongly interacting regimes near unitarity that include full fluctuations[134–136].

The SPT approach offers an alternative, straightforward way to estimate the critical temperature across the entire transition. Using the Pauli principle, the first excited state above the ground state can be determined along the transition. This excited state involves single-particle excitations while the ground state is composed of only phonon normal modes. The difference between these

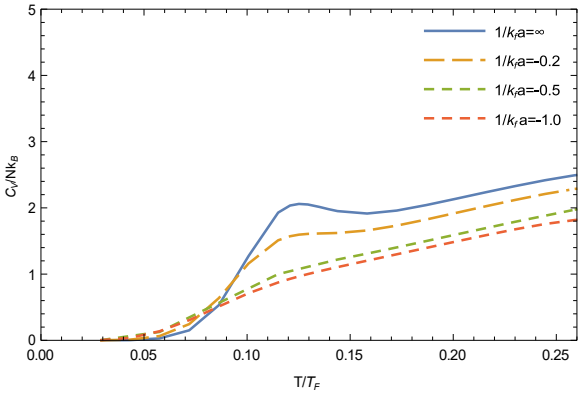

Fig. 5 The heat capacity showing the softening of the cusp as the interparticle interaction decreases from a maximum at unitarity: blue line $1/k_f a = \infty$; orange dashed line $1/k_f a = -0.02$; green dotted line $1/k_f a = -0.5$; red dot dashed line $1/k_f a = -1.0$.

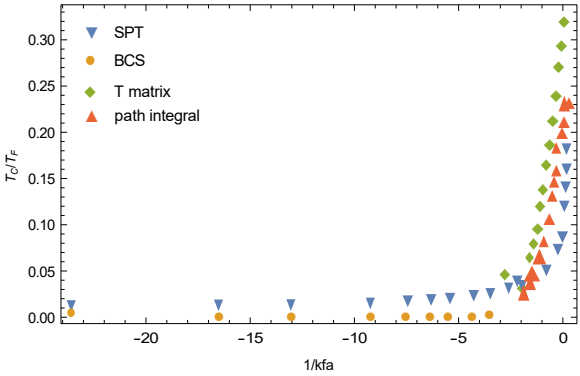

Fig. 6 The critical temperature, T_C/T_F as a function of $1/k_f a$ for 30 fermions compared to the BCS prediction ($T_C/T_F = 0.277 \exp(\pi/(2k_f a))$ valid for $1/k_f a \ll -1.0$ and theoretical results: T matrix[134] and path integral[135] for $-1.0 \leq 1/k_f a \ll 0$.

two states provides an estimate of the critical temperature as simply the temperature equivalent: $E_{ex} - E_{gs} = k_B T_C$. This estimate is graphed in Fig. 6 normalized by the Fermi temperature T_F, $E_F = (3N)^{1/3} n\omega_{ho} = k_B T_F$, and compared to other theoretical results in the region near unitarity and to the BCS expression, $T_C/T_F = 0.277 \exp(\pi/(2k_f a)$ valid for $1/k_f a \ll -1.0$. The SPT results are slightly higher than the BCS results, showing a gradual increase from the deep BCS regime toward unitarity and then a rapid increase for $1/k_f a \geq -1.0$ as the interactions approach unitarity. The curve converges at unitarity at $(T/T_F)_C = 0.18$ in reasonable agreement with several other theoretical approaches[122, 128, 130–132]

3.4 The breathing mode frequency from BCS to Unitarity.

The investigation of collective excitation modes has long been used to gain insight into the behavior of many-body systems. The excitation frequencies of ultracold Fermi gases have been studied intensely across the BEC-BCS transition. The radial compression or "breathing" mode in a cylindrical potential has been of particular interest due to a surprising feature observed in the regime of strong interactions, specifically an abrupt decrease in the frequency near unitarity[4, 137–139]. This minimum has been confirmed theoretically[140–142].

The microscopic basis for this minimum in the breathing mode has been attributed to the formation of Cooper pairs as unitarity is approached which decreases the frequency as the gas becomes more compressible[142]. It has also been suggested from the observation of this minimum coupled with an analysis of the corresponding damping time, that this feature could be a signature of a transition from a superfluid to a collisionless phase[4, 137–139] as interactions weaken toward the independent particle regime.

In my earlier study of the SPT frequencies, both radial frequencies had a broad minimum as a function of the interparticle interaction strength parameter, V_0[19]. To compare to existing results in the literature, I have graphed in Fig. 7 the SPT radial breathing frequency ω_{0-} as a function of the parameter $1/N^{1/6}a$ through the region of the minimum. This figure clearly shows a minimum for the SPT frequency between $1/N^{1/6}a = -1.0$ and unitarity, $1/N^{1/6}a = 0$, in close agreement with the previous experimental and theoretical results[4, 138, 140–142]. The SPT minimum is broad in Fig. 2 in Ref. [19] graphed as a function of V_0 on a log scale spanning several orders of magnitude from $V_0 = 10^{-3}$ to $V_0 = 1.0$, but is quite sharp when graphed as a linear function of $-1/N^{1/6}a$ in Fig. 7 where it maps into a small region between $1/N^{1/6}a = -1.0$ and $1/N^{1/6}a = 0$.

When the other SPT radial excitation, ω_{1-}, which is a single-particle excitation is plotted as a function of $1/N^{1/6}a$, its minimum is visible, but quite small.

The analytic form of the SPT normal modes offers an opportunity to analyze the microscopic dynamics responsible for this minimum thus offering an alternative to previous suggestions involving Cooper pairing or transitioning to a collisionless regime. By tracking the contribution of different terms in the Hamiltonian to the analytic expression for the frequency across the transition, one can understand what is happening microscopically in this approach to produce this minimum.

Understanding the microscopic dynamics of the minimum in the radial breathing frequency.. An analysis of the radial breathing frequency ω_{0-} is given in Appendix C in Ref. [19] in terms of the FG matrix elements from the first-order Hamiltonian terms (Eq. (13)). The formula derived in this Appendix for ω_{0-} in terms of the FG elements is:

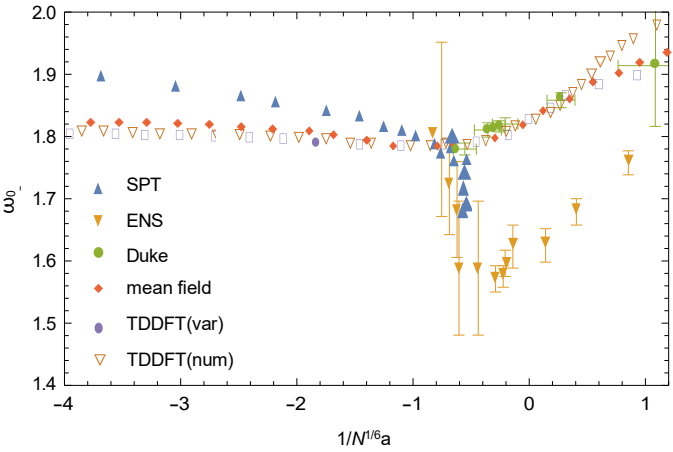

Fig. 7 Excitation frequency for the radial breathing mode in a symmetric trap as a function of $1/N^{1/6}a$ for 30 fermions showing the minimum as unitarity is approached that is seen theoretically: mean field[142], TDDFT(var)[140], TDDFT(num)[141] and experimentally in cylindrical traps: ENS[138] and Duke[4]

$$\omega_{0-} \approx \sqrt{G_a F_a + (N-1) G_a F_b} \tag{19}$$

where $G_a = 1$, F_a and F_b involve derivatives of V_{eff} (See Eq. 9.) which is a sum of the confining potential V_{conf}, centrifugal potential $V_{\text{cent}} = U$, and interparticle interaction potential V_{int}:

$$V_{\text{eff}} = U + V_{\text{conf}} + V_{\text{int}}. \tag{20}$$

yielding three terms for F_a: $F_a = F^{\text{conf}}_a + F^{\text{cent}}_a + F^{\text{int}}_a$ and one nonzero term for F_b involving the interaction potential: $F_b = F^{\text{int}}_b$. The term F^{conf}_a is a constant equal to 1. All the terms are explicitly defined in Appendix B in Ref. [19].

As in the analysis of the angular frequencies in Section VI of Ref. [19], it is useful to track the magnitude of γ_∞, the angle cosine of each pair of particles at the minimum of the maximally-symmetric structure at large dimension. Early dimensional scaling work identified a nonzero value of this parameter as a signature of the existence of correlation between the particles. Mean-field results have $\gamma_\infty = 0$ corresponding to no correlation between the particles, while increasing values of γ_∞ indicated stronger and longer-range correlation effects.

Consider the independent particle limit, i.e. collisionless regime, with no interparticle interactions so $V_0 = 0$ and thus no correlations between the particles i.e. $\gamma_\infty = 0$ so only the harmonic trap is affecting the particles which, of course, are also obeying the Pauli principle. Most terms in the expression for ω_{0-} in Eq. (19) are zero. The only nonzero terms are $F^{\text{conf}}_a = 1$ from the trap potential and $F^{\text{cent}}_a = 3$ which originates in the kinetic energy, giving $F_a = 4$, $F_b = 0$ so $\omega_{0-} = 2\omega_{ho}$ as expected and confirmed in the laboratory. (See Appendix F in Ref. [19].) As interactions are introduced, γ_∞ assumes a small nonzero value, signaling the existence of weak correlations. This nonzero value

means that all terms in the expression for $\bar{\omega}_{0-}$ are nonzero. F_a^{cent} begins to decrease, while F_a^{int} and F_b^{int} increase. Along the BCS to unitarity transition, the value of $\bar{\omega}_{0-}$ is a balance between the centrifugal term which is decreasing and the interaction terms which are increasing as interactions ($\bar{V}_0$) and correlations (γ_∞) both increase from BCS toward unitarity. The minimum in the frequency occurs from the continued decrease in the centrifugal terms just before the increase in the interaction terms dominates.

Microscopically, one can understand what is happening based on this analysis of the Hamiltonian terms. The increase in the correlated motion of the particles as tracked by the increase in γ_∞ minimizes the interparticle interactions resulting in slower oscillations of the breathing mode. Eventually the increase in $\bar{V}_0$, i.e. the increased strength of the interparticle interactions will lead to more rapid oscillations i.e. an increase in the frequency as unitarity is approached. The gradual decrease observed when $\bar{\omega}_{0-}$ is plotted as a function of $\bar{V}_0$ in Ref. [19] appears as a sudden, quite narrow dip in the frequency when graphed as a function of $1/(N^{1/6}a)$. This is due to the rapidly changing scattering length in this region as unitarity is approached. In summary, the minimum can be understood as the result of two competing factors that affect the microsopic behavior without invoking Cooper pairs: the increase in correlation which minimizes the interparticle interactions thus slowing down the frequency of the oscillations and second, the increasing strength of the interparticle interactions which eventually dominates and speeds up the frequency.

4 Discussion and Conclusions

In this study, I explored the ability of normal modes to describe the behavior of ultracold Fermi gases including superfluidity across the BCS to unitarity transition without assuming Cooper pairing. In particular, I calculated the following observables: ground state energies, thermodynamic entropies, critical temperatures and the radial breathing frequency across this transition using normal modes and compared to available experimental and theoretical results.

This study has yielded close agreement with both experimental and theoretical results for the ground state energies, thermodynamic entropies and critical temperatures at weaker interactions away from unitarity. These calculations tested the lowest frequencies relevant to ultracold systems as well as the spectrum of frequencies needed for the partition function. In all of these calculations, the Pauli principle plays a central role in choosing the states that contribute to these properties. The final study involved a single frequency, the breathing frequency, which did not contribute to the earlier studies due to its larger value. The observed dip in this SPT frequency near unitarity was in close agreement with results first observed in the laboratory and later confirmed theoretically, suggesting that the frequencies produced by this first-order SPT Hamiltonian are based on microscopic dynamics that produce observable effects.

The normal coordinates constitute beyond-mean-field, analytic solutions to a many-body Hamiltonian and offer microscopic insight into the evolution of properties across the BCS to unitarity transition. The analytic forms for the frequencies and coordinates allow a detailed look at the dynamics by tracking the effect of the Hamiltonian terms across the transition. As correlations increase toward unitarity as tracked by the parameter γ_∞, the dependence of properties on the details of the interparticle interactions is minimized consistent with the universal behavior which is also seen at the independent particle limit. The Pauli principle, of course, is dominating the dynamics at both limits underpinning the universal behavior in these regimes.

The results of this study are based on an exact solution of the first-order equation of SPT perturbation theory which contains beyond-mean-field effects. Higher-order terms that have been formulated, but not implemented, are not included. These terms could become significant in some regimes changing the dynamics. The SPT formalism also does not offer a mechanism for the two-body pairing that occurs as the ensemble transitions to the BEC regime.

The successful determination of these properties across the BCS to unitarity transition using these first-order solutions supports a normal mode description of superfluidity with a clear picture of the evolving microscopic dynamics across a broad range of interparticle interaction strengths and represents an interesting alternative to Cooper pairing models.

Declarations

- Funding

  I am grateful to the National Science Foundation for financial support under Grant No. PHY-2011384.

- Competing interests

  The author has no conflicts of interests to declare that are relevant to the content of this article. The author has no relevant financial or non-financial interests to disclose.

- Compliance with Ethical Standards

  The author has no potential conflicts of interest.

- Consent for publication

  Not applicable

- Data Availability

  The data generated or analysed during this study are available from the author on reasonable request.

- Code Availability

  Not applicable

- Authors' contributions

  D.K. Watson, as the sole author, was responsible for the design of this research, the investigation, writing the original draft of the manuscript and editing the final draft.

References

[1] M. Greiner, C.A. Regal, and D.S. Jin, Nature 426, 537(2003).

[2] M.W. Zwierlein, C.A. Stan, C.H. Schunck, S.M.F. Raupach, S. Gupta, Z. Hadzibabic, and W. Ketterle, Phys. Rev. Lett. 91, 250401 (2003).

[3] S. Jochim, M. Bartenstein, A. Altmeyer, G. Hendl, S. Riedl, C. Chin, J. Hecker Denschlag, R. Grimm, Science 302, 2101 (2003).

[4] J. Kinast, S.L. Hemmer, M.E. Gehm, A. Turlapov and J.E. Thomas, Phys. Rev. Lett. 92, 150402 (2004).

[5] T. Bourdel, L. Khaykovich, J. Cubizolles, J. Zhang, F. Chevy, M. Teichmann, L. Tarruell, S.J.J.M.F. Kokkelmans and C. Salomon, Phys. Rev. Lett. 93, 050401 (2004).

[6] C.A. Regal, M. Greiner, and D.S. Jin, Phys. Rev. Lett. 92, 040403(2004).

[7] M.W. Zwierlein, C.A. Stan,C.H. Schunck,S.M.F. Raupach, A.J. Kerman, and W. Ketterle, Phys. Rev. Lett. 92, 120403(2004).

[8] C. Chin, M. Bartenstein, A. Altmeyer, S. Riedl, S. Jochim, Hecker-Denschlag and R. Grimm, Science 305, 1128 (2004).

[9] G.B. Partridge, K.E. Strecker, R.I. Kamar, M.W. Jack and R.G. Hulet, Phys. Rev. Lett. 95, 020404 (2005).

[10] J. Bardeen, L.N. Cooper, and J.R. Schrieffer, Phys. Rev. 108, 1175 (1957).

[11] A.J. Leggett, In *Modern Trends in the Theory of Condensed Matter. Proceedings of the XVIth Karpacz Winter School of Theoretical Physics, Karpacz, Poland*, pgs. 13-27, Springer-Verlag, Berlin, 1980.

[12] A.J. Leggett, Rev. Mod. Phys. 73, 307(2001).

[13] D.M. Eagles, Phys. Rev. 186, 456 (1969).

[14] P. Nozieres and S. Schmitt-Rink, J. Low Temp. Phys .59, 195 (1985).

[15] S. Giorgini, L.P. Pitaevskii, and S. Stringari, Rev. Mod. Phys. 80, 1215(2008).

[16] M. Randeria and E. Taylor, Ann. Rev. Condensed Matter Phys. 5, 209(2014).

[17] D.K. Watson, Phys. Rev. A 92, 013628 (2015).

[18] D.K. Watson, J. Phys. B. 52, 205301 (2019).

[19] D.K. Watson, Phys. Rev. A 104, 033320 (2021).

[20] D.L. Rousseau, R.T. Bauman, S.P.S. Porto, J. Ramam Spect., 10, 253(1981).

[21] K. D. Kokkolas, Class. Quantum Grav. 8, 2217 (1991).

[22] M.J. Clement, App J. 249, 746(1981).

[23] N. Zagar, J. Boyd, A. Kasaara, J. Tribbia, E. Kallen, H. Tanaka, and J.-i Yano, Bull. Am. Meteor. Soc. 97 (2016).

[24] S.C. Webb, Geophys.J. Int. 174, 542(2008).

[25] B.V. Sanchez, J. Marine Geodesy 31, 181(2008).

[26] J. Lee, K.T. Crampton, N. Tallarida, and V.A.Apkarian, Nature 568, 78(2019).

[27] L. Fortunato, EPJ Web of Conferences 178, 02017 (2018).

[28] E.C. Dykeman and O.F. Sankey, J. Phys.:Condens. Matter 22, 423202(2010).

[29] M. Coughlin and J. Harms, arXiv:1406.1147v1 [gr-qc] (2014).

[30] R.M. Stratt, Acc. Chem. Res. 28, 201(1995).

[31] C.R. McDonald, G. Orlando, J.W. Abraham, D. Hochstuhl, M. Bonitz, and T. Brabec, Phys. Rev. Lett. 111, 256801 (2013); F. Dalfovo, S. Giorgini, L.P. Pitaevskii, and S. Stringari, Rev. Mod. Phys. 71, 463(1999); D. Jaksch, C. Bruder, J.I. Cirac, C.W. Gardiner, and P. Zoller, Phys. Rev. Lett. 81, 3108(1998); H. Dong, W. Zhang, L. Zhou and Y. Ma, Sci. Rep. 5, 15848; doi: 10.1038/srep15848(2015).

[32] H.C. Nagerl, C. Roos, H. Rohde, D. Leibfried, J. Eschner, F. Schmidt-Kaler and R. Blatt, Fortschr. Phys. 48, 623 (2000).

[33] B.A. McKinney, M. Dunn, D.K. Watson, and J.G. Loeser, Ann. Phys. 310, 56 (2003).

[34] M. Dunn, D.K. Watson, and J.G. Loeser, Ann. Phys. (NY), 321, 1939 (2006).

[35] W.B. Laing, M. Dunn, and D.K. Watson, J. of Math. Phys. 50, 062105 (2009).

[36] W.B. Laing, M. Dunn, and D.K. Watson, Phys. Rev. A 74, 063605 (2006).

[37] W.B. Laing, D.W. Kelle, M. Dunn, and D.K. Watson, J Phys A 42, 205307 (2009).

[38] M. Dunn, W.B. Laing, D. Toth, and D.K. Watson, Phys. Rev A 80, 062108 (2009).

[39] G. t'Hooft, Nucl. Phys. B72, 461(1974);B75(1974).

[40] K.G. Wilson, Phys. Rev. Lett. 28, 548 (1972); Rev. Mod. Phys. 55, 838 (1983).

[41] G. Chen, Z. Ding, C.-S. Lin, D. Herschbach, M.O. Scully, J. Math. Chem. 48, 791(2010).

[42] A.Svidzinsky, G. Chen, S. Chin, M. Kim, D. Ma, R. Murawski, A. Sergeev, M. Scully, D. Herschbach, International Reviews in Physical Chemistry, 27, 665 (2008).

[43] D.R. Herrick, J. Math. Phys. 16, 281(1975).

[44] J.G. Loeser, J.H. Summerfield, A.L. Tan, and Z. Zhang, J. Chem.Phys. 100,5036(1994).

[45] S. Kais and D.R. Herschbach, J. Chem. Phys. 100, 4367(1994).

[46] J.G. Loeser, J. Chem. Phys. 86, 5635(1987).

[47] D.R. Herschbach, J.G. Loeser, and W.L. Virgo, J. Phys. Chem. A 121, 6336 (2017).

[48] W.L. Virgo, D.R. Herschbach, Chem. Phys. Lett. 634, 179(2015).

[49] P.F. Loos, P.M.W. Gill, Phys. Rev. Lett. 105, 113001(2010).

[50] A. Svidzinsky, M.O. Scully, D. Herschbach, Phys. Today 66, 33 (2014).

[51] S. Kais, T.C. Germann and D.R. Herschbach, J. Phys. Chem. 98, 11015(1994).

[52] A. Svidzinsky, M.O. Scully, and D. R. Herschbach, Phys. Rev. Lett. 95, 080401 (2005).

[53] A. Chatterjee, J. Math. Phys. 41, 2515(2000).

[54] Y.P. Varshni, Can. J. Phys. 71, 122(1993).

[55] S.M. Sung and J.M. Rost, J. Phys. Chem. 97, 2479 (1993).

[56] S. Kais and P. Serra, Adv. Chem Phys. 125, 1(2003).

[57] V.S. Popov, and A.V. Sergeev, Phys. Lett A 172, 193(1993).

[58] V.S. Popov and A.V. Sergeev, Phys. Lett. A. 193, 165(1994).

[59] S. Kais and D. R. Herschbach, J. Chem. Phys. 98, 3990(1993).

[60] D.K. Watson and B.A. McKinney, Phys. Rev. A 59, 4091(1999).

[61] B.A. McKinnney and D.K. Watson, Phys. Rev. A 65, 033604(2002).

[62] B.A. McKinney, M. Dunn, D.K. Watson, Phys. Rev. A 69, 053611 (2004).

[63] M. Y. Veillette, D.E. Sheehy and L. Radzihovsky, Phys. Rev. A 75, 043614 (2007).

[64] Y. Nishida and D. T. Son, In W. Zwerger, editor, *The BCS-BEC Crossover and the Unitary Fermi Gas*, Lecture Notes in Physics, Springer, 2011.

[65] Y. Nishida and D. T. Son, Phys. Rev. Lett. 97, 050403 (2006).

[66] Y. Nishida and D. T. Son, Phys. Rev. A 75, 063617 (2007).

[67] P. Zhang, H.-C. Long, C.-S. Jia, Eur. Phys. J. Plus 131, 117(2016).

[68] Y. Sun, G.-D. Zhang. C.-S. Jia, Chem. Phys. Lett. 636, 197 (2015).

[69] B. Roy and R. Roychoudhury, J. Phys. A 23, 3555(1990).

[70] A. Gonzalez, G. Loyola and M. Moshinsky, Rev. Mex. Fis. 40, 12 (1994).

[71] A. Chatterjee, Phys. Rep. 186, 249(1990).

[72] E. Whitten, Nucl. Phys. B 149, 285(1979).

[73] A. Gonzalez, Few Body Systems 10, 43(1991).

[74] E. Whitten, Phys. Today 33(7), 38(1980).

[75] G. t'Hooft, "Large N", arXiv:hep-th/0204069v1, (2002).

[76] C.J. Ahn, J. High Energy Physics 125(2011).

[77] C. Rim and W.I. Weisberger, Phys. Rev. Lett. 53, 965 (1984).

[78] C. Bender and S. Boettcher, Phys. Rev. D 51, 1875(1995).

[79] M. Horacsu, K. D. Rothy, B. Schroer, Nuclear Physics B 164, 333(1980).

[80] "The Large N Expansion in Quantum Field Theory and Statistical Physics", E. Brezin and S.R. Wadia, eds. World Scienfific Publ. Co, 1993.

[81] K. Capelle and L.N. Oliveira, Phys. Rev B 73, 113111 (2006).

[82] W. Metzner and D. Vollhardt, Phys. Rev Lett. 62, 324(1989).

[83] K. G. Wilson and J. Kogut, Phys. Rev. C 12, 75 (1974).

[84] S. Boettcher and M. Moshe, Phys. Rev. Lett. 74, 2410(1995).

[85] C.M. Bender, S. Goettcher and L. R. Mead, J. Math. Phys. 35, 368 (1994).

[86] D.K. Watson, Phys. Rev. A 93, 023622 (2016).

[87] D.K. Watson, Phys. Rev. A 96, 033601(2017).

[88] Y. K. Liu, M. Christandl, and F. Verstraete, Phys. Rev. Lett. 98, 110503 (2007).

[89] A. Montina, Phys. Rev. A 77, 022104 (2008).

[90] D.K. Watson and M. Dunn, Phys. Rev. Lett. 105, 020402 (2010).

[91] D.K. Watson and M. Dunn, J. Phys. B 45, 095002 (2012).

[92] W.B. Laing, M. Dunn, and D.K. Watson, EPAPS Document Number E-JMAPAQ-50-031904.

[93] *Dimensional Scaling in Chemical Physics*, edited by D.R. Herschbach, J. Avery, and O. Goscinski (Kluwer, Dordrecht, 1992).

[94] *New Methods in Quantum Theory*, edited by C. A. Tsipis, V. S. Popov, D. R. Herschbach, and J. Avery, NATO Conference Book, Vol. 8. (Kluwer Academic, Dordrecht, Holland).

[95] J.G. Loeser, J. Chem. Phys. 86, 5635 (1987).

[96] S. Kais and D.R. Herschbach, J. Chem. Phys. 100, 4367 (1994).

[97] S. Kais and R. Bleil, J. Chem. Phys. 102, 7472 (1995).

[98] D.K. Watson, Ann. Phys. 419, 168219 (2020).

[99] S.K. Adhikari, Phys. Rev. A 79, 023611(2009).

[100] X.-J. Liu, H. Hu,and P.D. Drummond, Phys. Rev. Lett. 102, 160401 (2009).

[101] X.-J. Liu, H. Hu, and P.D. Drummond, Phys. Rev. A 82, 023619 (2010).

[102] X.-J. Liu, H. Hu, and P.D. Drummond, Phys. Rev. B 82, 054524 (2010).

[103] T. Grining, M. Tomza, M. Lesiuk, M. Przybytek, M. Musial, R. Moszynski, M. Lewenstein, and P. Massignan, Phys. Rev. A 92, 061601(R) (2015).

[104] D. Blume, Physics 3, 74 (2010).

[105] D.Blume, Rep. Prog. Phys. 75, 046401 (2012).

[106] J. Levinsen, P. Massignan, S. Endo, and M.M. Parish, J. Phys. B 50, 072001 2017).

[107] J. Avery, D.Z. Goodson, D.R. Herschbach, Theor. Chim. Acta 81, 1 (1991).

[108] E. B. Wilson, Jr., J. Chem. Phys. 9, 76 (1941).

[109] E.B. Wilson, Jr., J.C. Decius, P.C. Cross, *Molecular vibrations: The theory of infrared and raman vibrational spectra*. McGraw-Hill, New York, 1955.

[110] M. Hamermesh, *Group theory and its application to physical problems*, Addison-Wesley, Reading, MA, 1962.

[111] See for example Ref. [109], Appendix XII, p. 347.

[112] L.D. Landau, "The Theory of a Fermi Liquid," Sov. Phys. 3, 920-925 (1956); "Oscillations in a Fermi Liquid," ibid. 5, 101-108 (1957).

[113] J. Carlson and S. Gandolfi, Phys. Rev. A 90 011601(R) (2014).

[114] S.K. Adhikari, Phys. Rev. A 79, 023611 (2009).

[115] D. Blume, J. von Stecher, and C.H. Greene, Phys. Rev. Lett. 99, 233201 (2007).

[116] S.Y. Chang and G. F. Bertsch, New J. Phys. 11, 023011 (2007).

[117] T. D. Lee et al., Phys. Rev. 105, 1119(1957).

[118] R. Jáuregui, R. Paredes, and G. Toledo Sánchez, Phys. Rev. A 76, 011604(R) (2007).

[119] J.T. Stewart, J.P. Gaebler, C.A. Regal and D.S. Jin, Phys. Rev. Lett. 97, 220406 (2006).

[120] D.T. Son, arXiv:0707.1851 [cond-mat.other], 2007.

[121] Q. Chen, J. Stajic, and K. Levin, Phys. Rev. Lett. 95, 260405 (2005).

[122] S. Nascimbene et al. Nature(London) 463, 1057(2010).

[123] H. Hu, X.-J. Liu, and P.D. Drummond, Phys. Rev. A 73, 023617 (2006).

[124] L. Luo, B. Clancy, J. Joseph, J. Kinast, and J. E. Thomas, Phys. Rev. Lett., 98,080402 (2007).

[125] L. Luo, J.E. Thomas, J. Low Temp. Phys. 154, 1 (2009).

[126] J.Kinast, A. Turlapov, J.E. Thomas, Q. Chen, J. Stajic, K. Levin, Science 307, 1296 (2005).

[127] M. J. H. Ku, A. T. Sommer, L. W. Cheuk, and M. W. Zwierlein, Science, 335(6068), 563-567 (2012).

[128] H. Hu, X.-J. Liu, and P.D. Drummond, New Journal of Physics 12, 063038 (2010).

[129] A. Bulgac, J.E. Drut, and P. Magierski, Phys. Rev. Lett 99, 120401 (2007).

[130] E. Burovski, N. Prokof'ev, B. Svistunov and M. Troyer, New J. of Phys. 8, 153 (2006).

[131] H. Hu, X.-J. Liu, and P.D. Drummond, Phys. Rev. A 77, 061605(R) (2008).

[132] R Haussmann and W Zwerger, Phys. Rev. A 78, 063602 (2008).

[133] E. Burovski, N. Prokof'ev, B. Svistunov and M. Troyer, Phys. Rev. Lett. 96, 160402 (2006).

[134] A. Perali, P. Pieri, L. Pisani, and G.C. Strinati, Phys. Rev. Lett. 92,220404 (2004).

[135] L. Dell'Anna and S. Grava, Condens. Matter 6,16(2021).

[136] C.A.R. S á de Melo, M. Randeria, and J. R. Engelbrecht, Phys. Rev. Lett. 71, 3202(1993).

[137] J. Kinast, A. Turlapov, and J.E. Thomas, Phys. Rev. A 70, 051401(R)(2004).

[138] R. Grimm, Proceedings of the International School of Physics "Enrico Fermi", Volume 164: Ultracold Fermi Gases, p 413-462, 2007.

[139] M. Bartenstein, A. Altmeyer, S. Riedl, S. Jochim, C. Chin, J. H. Denschlag, and R. Grimm, Phys. Rev. Lett. 92, 203201-1 (2004).

[140] Y.E. Kim and A.L. Zubarev, Phys. Rev. A 70, 033612(2004).

[141] N. Manini and L. Salasnich, Phys Rev. A 71, 033625(2005).

[142] H. Hu, A. Minguzzi, X-J Liu, and M.P. Tosi, Phys. Rev. Lett. 93, 190403(2004).